Supporting Information for Lab on a Chip

A cell rolling cytometer reveals the correlation between mesenchymal stem cell dynamic adhesion and differentiation state

Sungyoung Choi, Oren Levy, Mónica B. Coelho, Joaquim M.S. Cabral, Jeffrey M. Karp*, and Rohit Karnik*

I. Supplemental Materials and Methods

Materials

Recombinant human P-selectin, P-selectin/Fc chimera, E-selectin/Fc chimera, and recombinant IgG_1/Fc were purchased from R&D Systems (Minneapolis, MN). Human promyelocytic leukemia cell line (HL60), Iscove's modified Dulbecco's medium (IMDM), and fetal bovine serum were obtained from American Type Culture Collection (ATCC, Manassas, VA). Human mesenchymal stem cells (MSCs), MSC growth medium, MSC adipogenic differentiation medium, human osteoblasts, osteoblast growth medium, human subcutaneous preadipocytes, and preadipocyte growth medium-2 (PGM-2) were purchased from Lonza (Walkersville, MD). Oil red O, Fast Blue RP salt, and Naphthol AS-MX phosphate alkaline solution were obtained from Sigma-Aldrich (St. Louis, MO). Monoclonal antibodies were mouse antihuman anti-CD18, -CD24, -CD34, -CD43, -CD45, -CD73, -CD90, and -CD162 (BD Biosciences, San Jose, CA); -CD15s (Santa Cruz Biotechnology, Santa Cruz, CA); and -CD65 (eBioscience, San Diego, CA). Dulbecco's phosphate-buffered saline (DPBS) was supplied by Lonza. All other materials were obtained from BD Biosciences and Sigma-Aldrich, unless specified.

Cell culture and differentiation

All the cells were cultured at 37 °C in 5 % humidified CO_2 using specified culture medium. MSCs at passage numbers 3-7, osteoblasts at 2-5, and preadipocytes at 2-5 were used for experiments. For adipogenic differentiation of MSCs, the medium was switched to the MSC adipogenic differentiation medium. The medium was alternated twice or thrice per week between the adipogenic induction and maintenance media for 14 d. Osteogenic differentiation of MSCs was performed using the MSC culture medium supplemented with 10 nM dexamethasone (Millipore, Billerica, MA) for 14 d. Adipocyte induction of preadipocytes was performed for 7 d using the adipocyte differentiation media which was prepared by adding the preadipocyte growth medium-2 (PGM-2) SingleQuots™ (Lonza) of insulin, dexamethasone, indomethacin, and isobutyl-methylxanthine to 100 mL of PGM-2. Non-induced controls were kept in culture medium. For experiments, cell culture media was aspirated and the flask washed with DPBS. Cells were detached using Accutase cell detachment solution (BD Biosciences). The cells were then washed twice and re-suspended in DPBS or culture medium. Cell samples were filtered with 30 µm celltrics filter (Partech, Germany) to remove cell aggregates before running the experiments.

For enzymatic inhibition experiments, the detached MSCs were treated with 120 µg/mL *O*-glycoprotease (Accurate Chemical and Scientific Corporation, Westbury, NY) or 100 U/mL neuraminidase (New England BioLabs, Ipswich, MA) for 30 min at 37 °C. Untreated controls were kept in 1% BSA solution under the same conditions. Efficiency of enzyme treatment was examined by staining of enzyme-treated and untreated HL60 cells, which have known receptors that contain *O*-linked sialoglycoproteins (*i.e.* CD43) or sialic acid residues (*i.e.* CD15s), and

subsequent flow cytometric analysis, leading to a significant reduction in fluorescence intensity after enzyme treatment (Figure S8).[s1,s2]

Flow cytometry analysis was performed using a fluorescence-activated cell sorter (FACS; Accuri Cytometers, Inc., MI). MSCs expressed high level MSC markers CD73 and CD90 (> 99% cells), while they did not express hematopoietic markers CD34 and CD45, and receptors which are known to have a binding affinity to E-selectin (Figure S6).

The cell viability was determined by trypan blue, and was 96.2 ± 2.1%, 89.7 ± 3.5%, and 91.0 ± 1.6% for un-treated MSCs, enzyme-treated MSCs, and the cells differentiated from MSCs, respectively. The viability of osteoblasts, preadipocytes, and adipocytes which were differentiated from preadipocytes was 97.0 ± 3.0%, 96.0 ± 2.0%, and 91.2 ± 1.0%, respectively.

Histochemical staining was performed to examine cell differentiation. Cells were rinsed with DPBS, fixed with 4% paraformaldehyde, and carefully washed with deionized water. Fixed cells were stained with probing solutions (Oil Red O or alkaline phosphatase) and then washed with deionized water. Osteoblasts were also identified based on positive staining for alkaline phosphatase activity.

Device design and fabrication

The cell rolling cytometer (CRC) has a stacked structure in which two poly(dimethylsiloxane) (PDMS)-channel layers with upper and lower ridges face each other (Figure 1). Each layer of PDMS was cast from microfabricated photoresist molds, and then aligned and bonded together. The molds were made by patterning SU-8 photoresist (Microchem Corp., Newton, MA). Two-step photolithography was used to define slant ridges on linear channels. The first layer of photolithography defined the main linear-channel structures; the second layer was aligned to lie on top of the channel structures in the first layer and defined the pattern of slant ridges. The focusing channel had 55 focusing ridges with $\theta = 40°$, $p_t = 35$ μm, and $p_r = 35$ μm (Figure S1). The adhesion channel comprised 15 adhesion ridges with $\theta = 40°$, $p_t = 63$ μm, and $p_r = 63$ μm (Figure S1). The channel height (h_c) and gap height (h_g) between the top and bottom ridges were determined by the following design rule. In the absence of adhesion interactions, the cells must be focused by hydrophoresis. For the cells to be focused by hydrophoresis, the channel dimensions should satisfy the following design guidelines: If the cell has a diameter d, the gap size (h_g) should typically be in $d < h_g < 5d$ and the total channel height (h_t) should satisfy $2h_g < h_t$.[s3,s4] With these criteria, the CRC for HL60 cells ($d = 11.7 \pm 1.5$ μm) was defined with $h_g = 25.8 \pm 0.2$ μm and $h_t = 87.6 \pm 1.4$ μm and the CRC for MSCs ($d = 19.1 \pm 5.1$ μm) was defined with $h_g = 36.1 \pm 0.1$ μm and $h_t = 100.9 \pm 2.7$ μm. If a cell (*i.e.* small HL60 cells in the CRC for MSCs) does not meet the criterion, it can deviate from the focusing trajectory and move back and forth between the focusing and gutter sides, following rotational flows. Since such cell can affect the gauge to determine the potential sorting efficiency of the rolling phenotype, lateral position, h_g needs to be customized for cell size. The flat chamber device was also formed in PDMS with a cross-section of $w \times h = 98$ μm × 1,000 μm.

Experimental setup and measurement

Cells (~8 to 30 cells/μL) were flowed into the devices using a syringe pump (KD Scientific Inc., Holliston, MA). Cell adhesion was recorded at 300 frames per second (fps) using a high-speed camera (EX-F1; CASIO, Japan) mounted on an inverted microscope (TE2000-U; Nikon, Japan). The transit time at which cells pass through the

adhesion channel was counted manually with a time resolution of 0.2 ms. The lateral position of cells at the end of the channel was measured using ImageJ software (NIH). For flat flow-chamber experiments, cells were allowed to settle down to the bottom for 5 min before applying the target shear stresses. The cells were considered non-interacting when they moved at the velocity of the flow, whereas cells moving at less than 50% of the velocity of the non-interacting cells were defined as interacting. Prior to each experiment, the channels were degassed in a vacuum chamber for 30 min, filled with 1.5 μg/mL P-selectin for HL60 cells and with 30 μg/mL E- or P-selectin/Fc for other cell types. After 3 h incubation at room temperature, the channels were washed with 1% bovine serum albumin.

Numerical simulation

Flow simulations were performed to calculate the shear stress on the slant ridges where cells can tether and roll, and to visualize streamlines in the channels. Commercial computational fluid dynamics software (CFD-ACE+; ESI, Huntsville, AL) was used to solve three-dimensional models (the focusing and adhesion channels of the CRC) in the "Flow Mode." No-slip boundary conditions were applied at the channel walls. The four different geometries of channel were used for simulation; the focusing channel for HL60 cells with w = 100 μm, h_g = 26 μm, and h_t = 88 μm; the adhesion channel for HL60 cells with w = 200 μm, h_g = 26 μm, and h_t = 88 μm (Figure S3); the focusing channel for MSCs with w = 100 μm, h_g = 36 μm, and h_t = 101 μm; and the adhesion channel for MSCs with w = 200 μm, h_g = 36 μm, and h_t = 101 μm.

II. Supplemental Discussion

Potential applications of the cell rolling cytometer

The cell rolling cytometer suggests that to maximize MSC targeting for cell therapy applications involving exogenous cell sources that are systemically infused, it will be critical to examine the rolling response and identify culture conditions that maximize rolling. The CRC is a potential quantitative tool for assessing the rolling response of MSCs and for detecting changes in MSC phenotype, which could be useful for ensuring MSC quality control that is critical for cell-based therapy. The CRC may also highlight differences in cell adhesion for sorting of more potent MSC populations for cell therapies, similar to that shown recently in the case of human pluripotent stem cells.[S5] The applicability of the CRC extends beyond MSCs, and could potentially introduce a new label-free quantitative method to characterize surface expression of a variety of cells and tissues.

III. Supplemental Figures

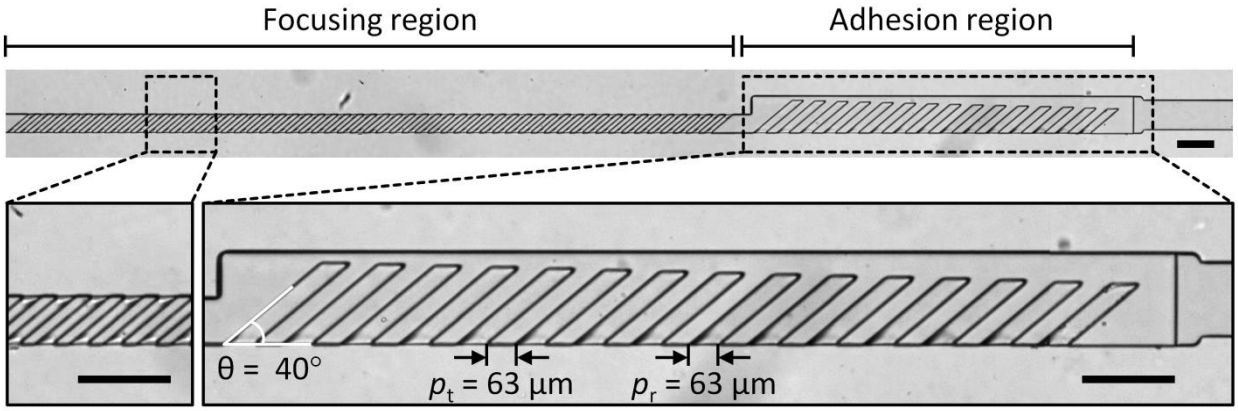

Figure S1. Micrographs of a cell rolling cytometer. Only one inlet is enough for device operation, since cell focusing autonomously occurs by hydrophoresis. This design enables effective cell capture in the adhesion region and quantification of dynamic adhesion at the single cell level. Scale bars, 200 µm.

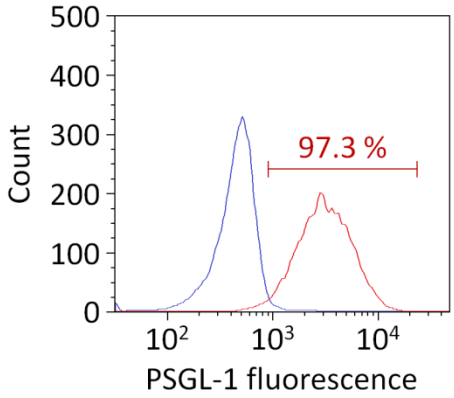

Figure S2. Flow cytometric analysis of P-selectin glycoprotein ligand-1 (PSGL-1) on HL60 cells. Blue line is isotype control, and red line is specific antibody.

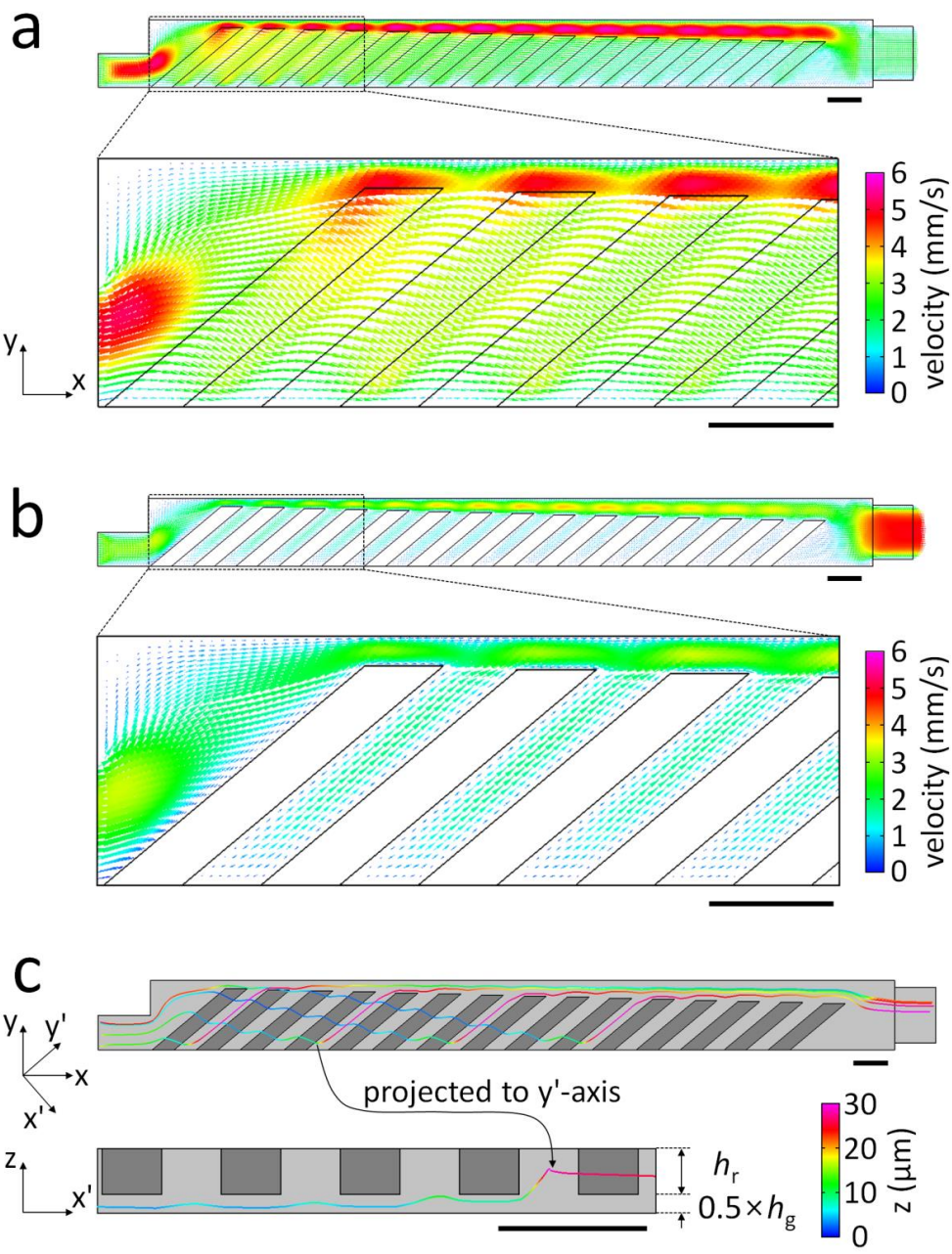

Figure S3. Flow simulations. (a,b) Simulated velocity vectors on *xy* cross-sections at positions of (a) z = 5 μm and (b) z = 28 μm, where the midplane of the channel was set to z = 0 μm. (c) Simulated streamlines around the top ridges. Because of geometry symmetry, only top half the channel is shown here. The side view image shows the streamline projected along the ridges, y'-axis. h_r is the height of the ridge. h_g is the gap between the top and bottom ridges. Scale bars, 100 μm.

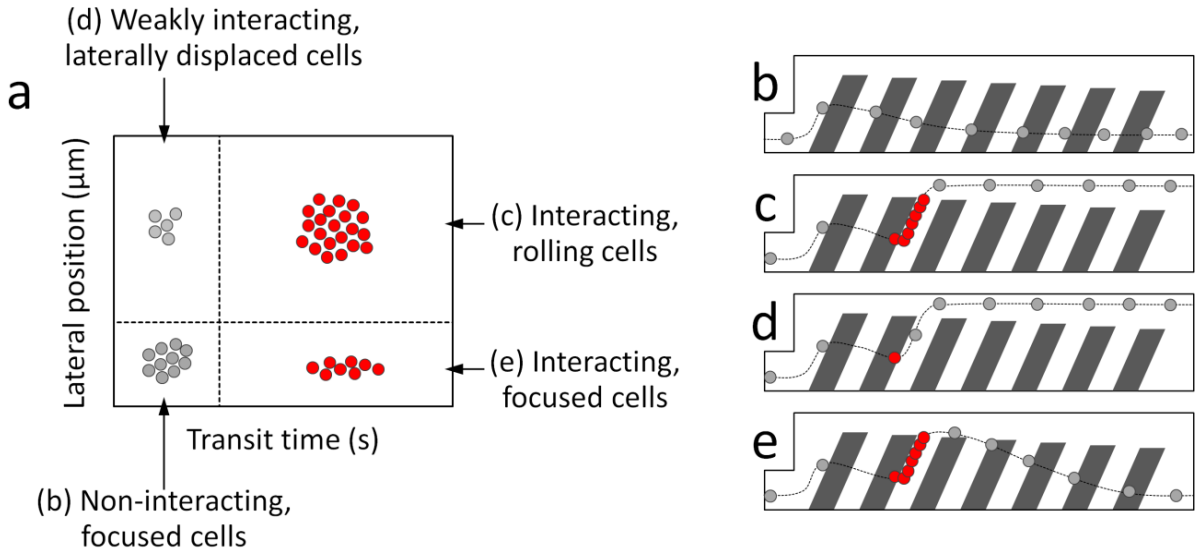

Figure S4. (a) Schematic scatter plot of the transit time and lateral position of a cell population which has the rolling phenotype. (b–e) Schematic trajectories of (b) non-interacting, focused, (c) interacting, rolling, (d) weakly interacting, laterally displaced, and (e) interacting, focused cells, respectively. Non-interacting, focused cells were in the left lower quadrant and rolling, interacting cells were mostly in the right upper quadrant. The left upper quadrant indicates weakly interacting cells that can tether to the surface and undergo lateral displacement, but are readily detached from the surface and therefore flow through quickly. The right lower quadrant represents a few interacting cells that undergo lateral displacement, but go back to the focusing side following the rotational flow. Transit time can be a gauge to determine whether a cell interacts with adhesion molecules, while lateral position can be a gauge to determine the potential sorting efficiency[s3] by the rolling phenotype.

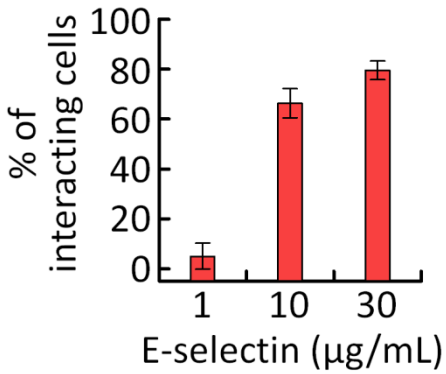

Figure S5. Effect of selectin incubation concentration on MSC rolling adhesion. Error bars show one standard deviation (n = 3).

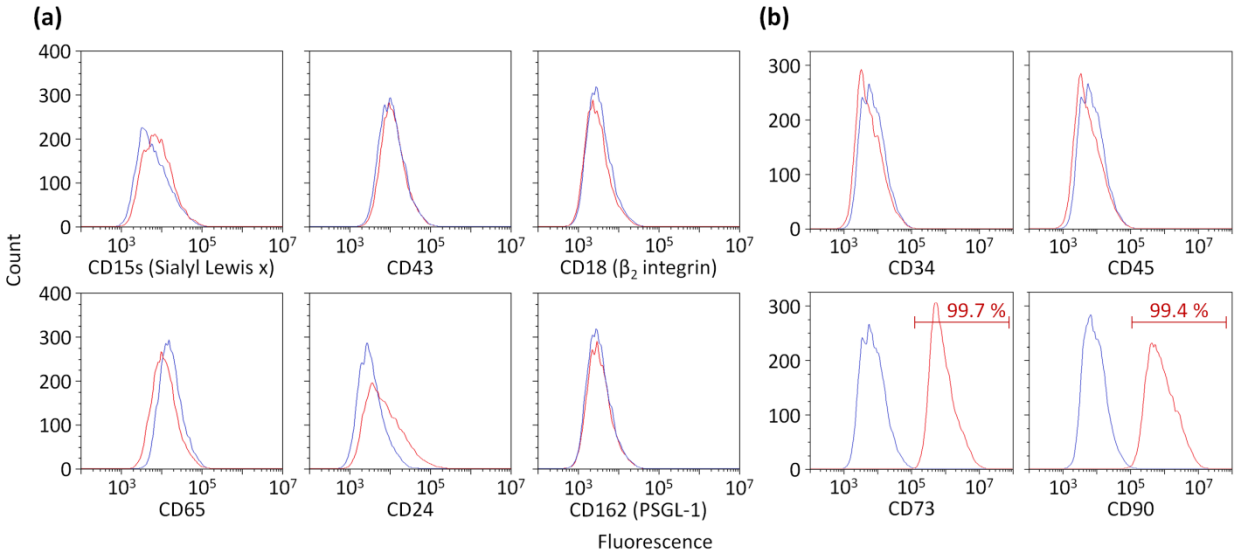

Figure S6. (a) Flow cytometric analysis of E-selectin ligand expression on human MSCs. (b) Immunophenotype of human MSCs. MSCs expressed high levels of mesenchymal markers (CD73 and CD90), while lacking hematopoietic markers (CD34 and CD45). Red lines represent target antibody reactivity and blue lines show the corresponding isotype control reactivity.

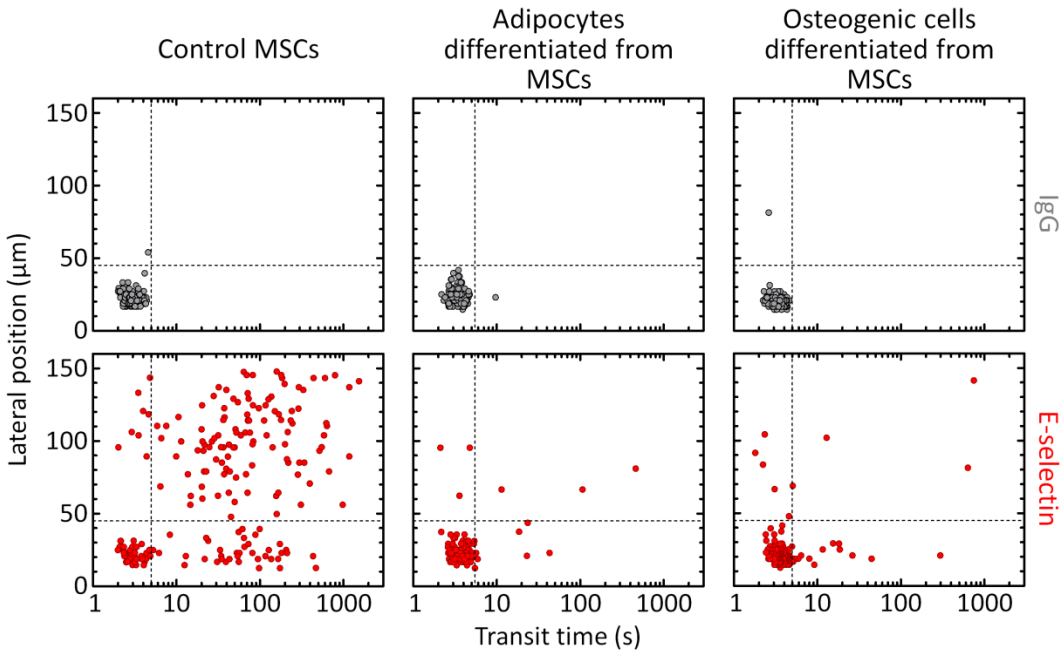

Figure S7. Scatter plots of the transit time and lateral position of 200 undifferentiated MSCs, adipocytes differentiated from MSCs, and osteogenic cells differentiated from MSCs in (Upper) IgG-passivated and (Lower) E-selectin coated channels.

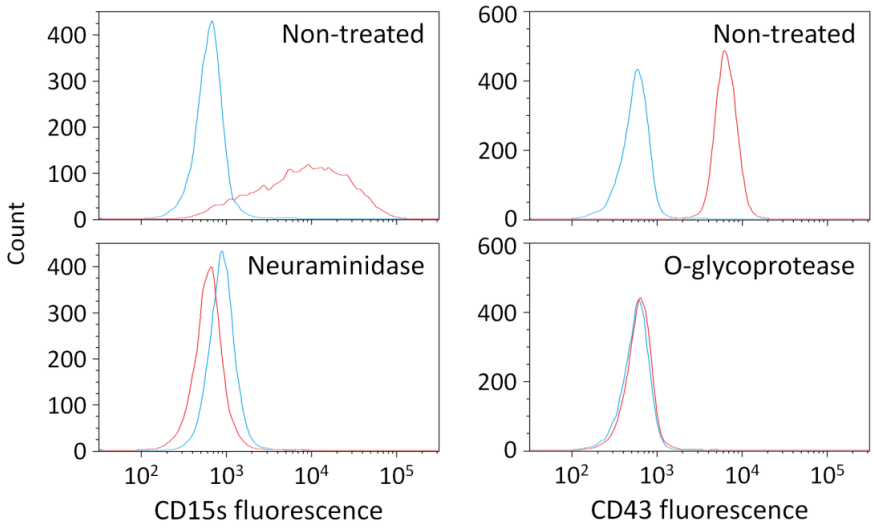

Figure S8. Flow cytometric analysis of enzyme-treated HL60 cells. Red lines represent target antibody reactivity and blue lines show the corresponding isotype control reactivity.

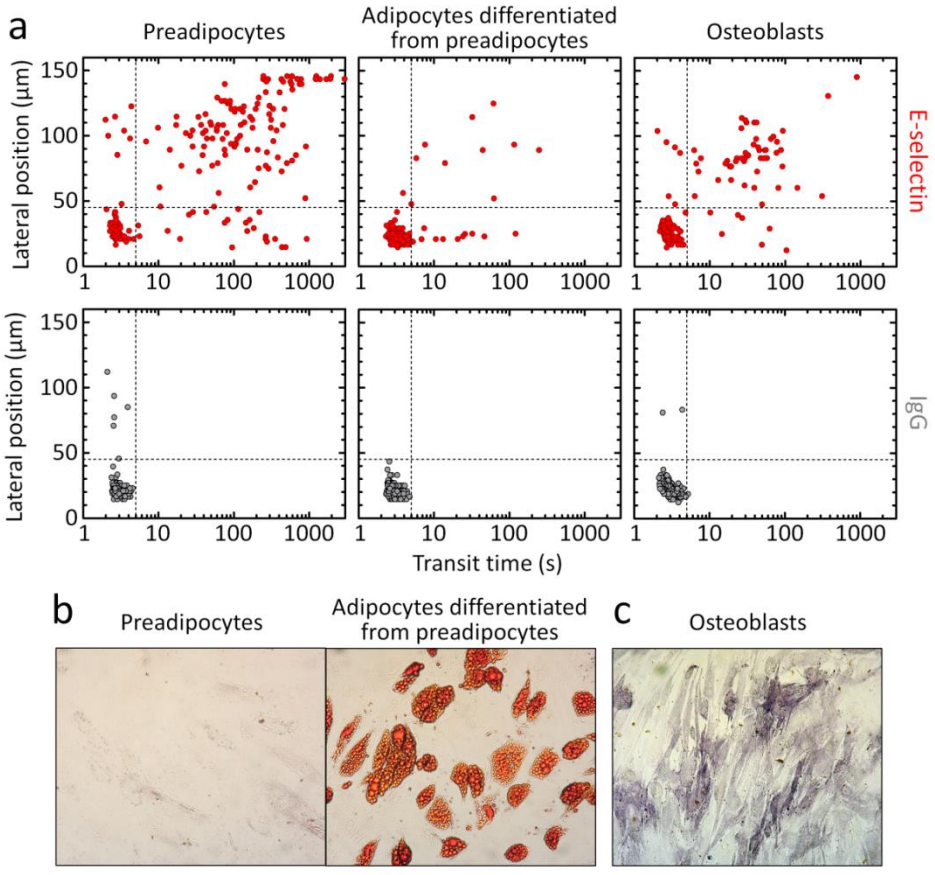

Figure S9. (a) Scatter plots of the transit time and lateral position of 200 preadipocytes, adipocytes differentiated from preadipocytes, and osteoblasts in (Upper) E-selectin-coated and (Lower) IgG-passivated channels. (b) Histochemical staining of preadipocytes and the adipocytes with Oil Red O stain. (c) Histochemical staining of osteoblasts with alkaline phosphatase stain.

IV. Video Captions

Video S1 Adhesion behavior of human MSCs in the E-selectin-coated channel at τ = 1.7 dyn/cm^2 and c_s = 30 μg/mL. This video was taken at 300 fps and then encoded with 50× playback speed (5× actual speed).

Video S2 Flowing behavior of human MSCs in the IgG-passivated channel at τ = 1.7 dyn/cm^2 and c_s = 30 μg/mL. This video was taken at 300 fps and then encoded with 50× playback speed (5× actual speed).

V. References

S1 D. R. Sutherland, K. M. Abdullah, P. Cyopick, A. Mellors, *J. Immunol* **1992**, *148*, 1458.

S2 S. Z. Gadhoum, R. Sackstein, *Nat. Chem. Biol.* **2008**, *4*, 751.

S3 S. Choi, J. M. Karp, R. Karnik, *Lab Chip* **2012**, *12*, 1427.

S4 S. Choi, J. -K. Park, *Small* **2009**, *19*, 2205.

S5 A. Singh, S. Suri, T. Lee, J. M. Chilton, M. T. Cooke, W. Chen, J. Fu, S. L. Stice, H. Lu, T. C McDevitt, A. J. García. *Nature Methods*, 2013, **10**, 438.